

## **MICROSTRUCTURED ELECTRODE ARRAYS FOR THIN FILM DEPOSITION**

Nina Lucas<sup>1\*</sup>, Philipp Sichler<sup>1</sup>, Christian Schrader<sup>2</sup>, Andreas Schenk<sup>2</sup>, Lutz Baars-Hibbe<sup>2</sup>,  
Stephanus Büttgenbach<sup>1</sup>, Karl-Heinz Gericke<sup>2</sup>

<sup>1</sup>Institut für Mikrotechnik, Technische Universität Braunschweig,  
Alte Salzdahlumer Straße 203, D-38124 Braunschweig, Germany

<sup>2</sup>Institut für Physikalische und Theoretische Chemie, Technische Universität Braunschweig,  
Hans-Sommer-Straße 10, D-38106 Braunschweig, Germany

\*Corresponding Author: Tel.: +49-531-391-9775; Fax: +49-531-391-9751  
E-mail: n.lucas@tu-bs.de

Keywords: Microstructured Electrodes, Atmospheric Pressure Plasma, Thin Film Deposition

### **Abstract**

Non-thermal plasma processing techniques have been established for a wide range of applications. Micro-structured electrode (MSE) arrays consist of an interlocked comb like electrode system with  $\mu\text{m}$ -gap widths. The electrode dimensions in the  $\mu\text{m}$ -range are realized by photolithography and galvanic techniques. These arrays are capable to generate large area uniform glow discharges up to atmospheric pressure. They are small enough to generate sufficiently high electric field strengths to ignite gas discharges applying only moderate radio frequency voltages (RF, 13.56 MHz, 80 V to 390 V in Ne, He, Ar and N<sub>2</sub>). One area of application for non-thermal plasma processing is thin film deposition. With the MSE arrays as plasma source some applications in the field of thin film deposition are investigated and found to produce adequate SiO<sub>2</sub> layers on various substrates. The properties of the layers are characterized by profilometry, ellipsometry, scanning electron microscopy and infrared spectroscopy.

### **Introduction**

Non-thermal plasma processing techniques optimized for atmospheric pressure applications are the subject of recently growing interest due to their significant industrial application potential. Thin film deposition at atmospheric pressure takes advantage of the high density of reactive species in the plasma providing high deposition rates while cost intensive vacuum equipment is avoided. There are many approaches published in the last 15 years to overcome the problems to generate and sustain stable uniform and homogenous non-thermal atmospheric plasma.

Massines et al. [1,2], Okazaki et al. [3,4], Trunec et al. [5] and Kelly-Wintenberg et al. [6] successfully generated atmospheric pressure glow discharges with a dielectric barrier array, and Park et al. [7,8] developed an atmospheric pressure plasma jet producing a stable and homogenous plasma. There are two approaches based on the Paschen similarity law ( $p \cdot d = \text{const.}$ ): Stark et al. [9,10], Penache et al. [11] and Eden et al. [12,13] use a micro hollow cathode array. We introduced micro-structured electrode arrays (MSE) consisting of an interlocked comb like electrode system with gap width of 70  $\mu\text{m}$  arranged on an insulating

surface [14-17]. Downscaling of the electrode dimensions to the  $\mu\text{m}$ -range and working in the Paschen minima of the different gases enables the ignition of discharges at atmospheric pressure and at moderate voltages. The essential advantage of MSE arrays is the capability to generate a homogenous plasma at atmospheric pressure. The presented MSE arrays are suitable plasma sources to treat surfaces of various sizes, because they use the advantages of small dimensions and may be individually adapted to the substrate size by modular scale up. This publication shows the deposition results of  $\text{SiO}_2$  layers on various substrates with different buffer gases.

### Processing of the MSE Arrays

Figure 1 shows an MSE array and the electrode gap design with a gap width of  $d = 70 \mu\text{m}$ . The processing of these arrays, already published in [18,19], was modified due to an improvement of throwing power during electrodeposition. For this reason sacrificial structures between the reactor structures which have to be removed after electrodeposition are no longer required. This leads to a simplification of the process. The MSE samples have an electrode width of  $1350 \mu\text{m}$  and the electrode thickness is  $70 \mu\text{m}$  in order to achieve high-pressure ranges. The base dimensions of the MSE samples are  $15 \times 15 \text{ mm}$ .

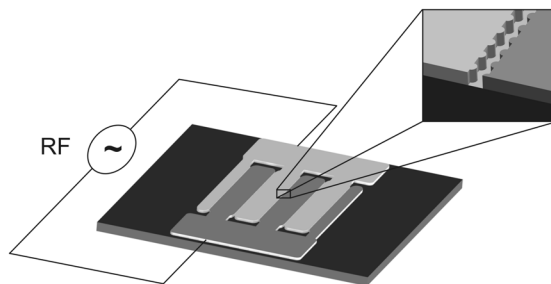


**Figure 1.** Scheme of a Microstructured Electrode array.

The plasma used for thin film deposition is of the non-thermal type. Nevertheless, the material used for the microstructured electrodes has to be thermally rugged. For this reason nickel is used as electrode material and electroplated on an alumina substrate. Therefore, a cleaned alumina wafer is sputter coated with three metallic layers. First, a  $90 \text{ nm}$  thick chromium layer is sputtered which works as adhesion layer for the following layers. Secondly,  $300 \text{ nm}$  copper which serves as seed layer for electroplating, and thirdly  $15 \text{ nm}$  chromium are sputtered on the wafer. The second chromium layer serves as optical absorption layer for the following SU-8 lithography, as protective coating for the copper and as adhesion layer for the SU-8. Subsequently a  $150 \mu\text{m}$  thick film of SU-8 photoresist [20, 21] is spun on the substrate. The SU-8 film is prebaked by heating at  $100 \text{ }^\circ\text{C}$  on a hotplate. After drying the SU-8 is exposed through a chrome mask with UV radiation to initiate crosslinking of the photoresist which is accelerated by a post-bake on a hotplate. The development of the SU-8 layer is done in  $\gamma$ -butyrolactone (GBL) and in propylen glycol monomethyl ether acetate (PGMEA) in a beaker with manual agitation. During development the non-polymerized resin is dissolved leaving a geometry complementary to the electrode design, serving as mould for the following electroplating. Residuals of the SU-8 layer are removed with a short descum in a  $\text{CF}_4\text{-O}_2$ -plasma ( $80 \text{ sccm O}_2$ ,  $20 \text{ sccm CF}_4$ ,  $100 \text{ W}$ ,  $4 \text{ minutes}$ ). Afterwards the second chromium layer is removed in a potassium ferricyanide ( $\text{K}_3[\text{Fe}(\text{CN})_6]$ ) solution. For electroplating a sulphamate-type bath (OMI Enthone Ni110 MicroFab;  $\text{pH} = 3,25$ ;  $50 \text{ }^\circ\text{C}$ ) with additives for reduction of residual stress is used. At  $15 \text{ mA cm}^{-2}$  for  $4 \text{ hours}$  and  $40 \text{ minutes}$  a thickness of  $70 \mu\text{m}$  is achieved with height deviations low enough to avoid grinding. Removal of the SU-8 layer after electroplating is achieved in an acetone bath at  $120 \text{ }^\circ\text{C}$  for  $24 \text{ hours}$ . Possible residuals after stripping are ashed in a barrel etcher with a  $\text{CF}_4\text{-O}_2$ -Plasma

(80 sccm O<sub>2</sub>, 20 sccm CF<sub>4</sub>, 300 W, 30 minutes). Afterwards the first chromium, the copper and the second chromium layer are etched to remove the remaining electric shortcut between the electrodes. Finally a 0.5 μm alumina layer is deposited on the structures, which serves as protective barrier.

## Experimental Setup

The thin film deposition setup is shown in figure 2. It consists of the MSE plasma source and an additional coplanar installed movable electrode plate at a variable distance of 2-9 mm. The additional coplanar installed electrode serves as carrier for the substrates and is biased with variable acceleration potentials (i.e. AC and pulsed DC voltages with various frequencies) to bridge the gap between the MSE and the substrate for the reactive species formed in the plasma. The acceleration potential signal is produced in a waveform generator (Stanford Research Systems, DS 345), afterwards amplified and finally transformed with a coil. The output signal can also be rectified with a high voltage diode in order to investigate AC and pulsed DC with both polarities.

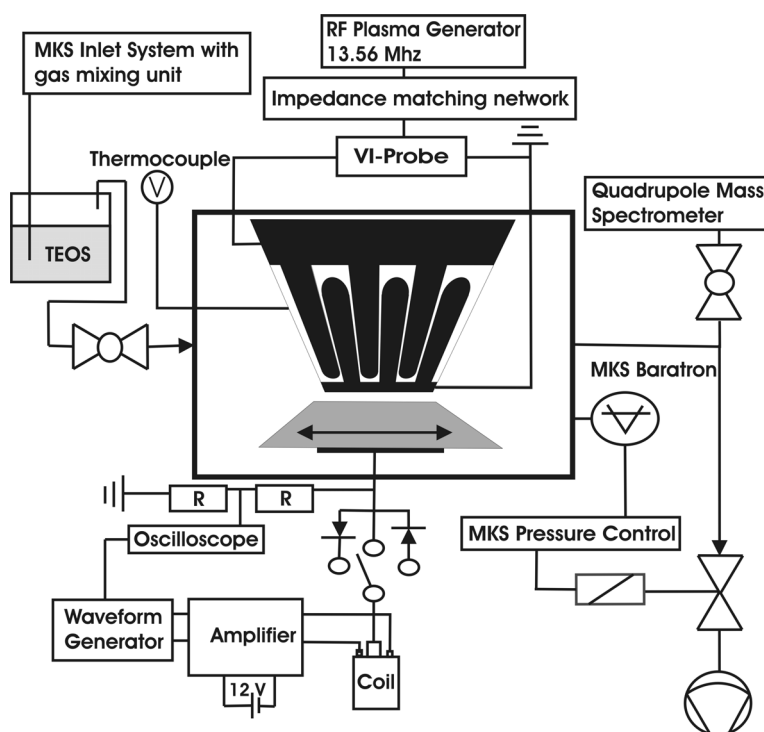


**Figure 2.** Schematic view of the experimental setup.

A K-type Chromel Alumel thermocouple is placed directly under the plasma source measuring the temperature rise during plasma operation. A gas flow rate between 1 sccm and 300 sccm can be set up by means of mass flow controllers. For online detection of the plasma product gases a differentially pumped quadrupole mass spectrometer (Pfeiffer Vacuum, QMS 200) is used. The discharges are generated using RF power supply at 13.56 MHz (ENI ACG-3B) equipped with a matching network (ENI, MW5D). Between the matching network and the plasma source a special probe is inserted in order to measure voltage, current and phase angle of the system.

## Deposition Results

To deposit SiO<sub>2</sub> layers on various substrates the precursor molecule tetraethoxysilane (TEOS) is used. This substance is added into the buffer gases (He, Ne, Ar and N<sub>2</sub>) with a bubbler as shown in figure 2. The feed gas with the precursor and 1 % of oxygen is conducted into the plasma

reactor with a fixed flow rate (100 sccm) by a gas mixing unit. The deposition experiments are tested on various substrates like polyethylene terephthalate (PET), polypropylene (PP), polystyrene (PS), copper and silicon with a similar deposition period of 300 s. The acceleration potential on the coplanary installed electrode in a distance of 6 mm to the plasma source is performed by a sine potential with  $f = 9.5$  kHz leading to a maximum voltage of 1800 Vpp. The applied RF power ranges from 22 W to 32 W in Ar and from 30 W to 35 W in nitrogen.

The results show no thermal damage of the substrates independent of the substrate material and the buffer gas. The deposition experiments lead to adhesive layers on PET, PS, copper and silicon with the buffer gas nitrogen up to 300 hPa and the buffer gas argon up to 600 hPa, respectively. The deposited layers are apparent by iridescence effects on the surface of the substrates. These effects are primarily visible at the boundaries of the area exposed to the plasma. The usage of helium and neon lead to non-adhesive amorphous powders. Polypropylene is not a suitable substrate for deposition experiments. The deposition experiments with polypropylene (PP) as substrate show non adhesive layers obtained in all applied buffer gases and pressures removable with 70 % ethanol solution. As confirmation IR spectra have been made approving the complete removal.

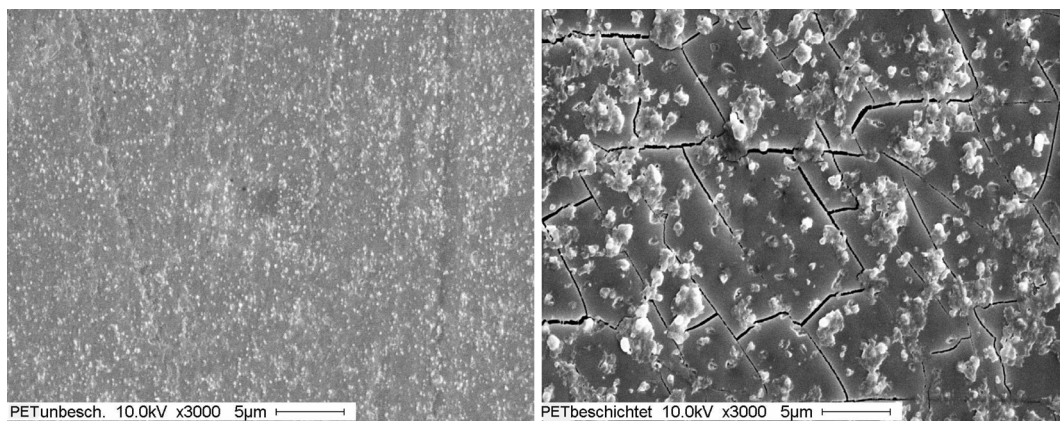


**Figure 3.** SEM pictures of a uncoated (←) and coated (→) PET substrate.

The obtained SEM pictures of an uncoated and coated PET substrate in figure 3 give further information about the surface properties with high resolution. After cleaning with 70 % ethanol solution the coated substrate illustrates interrelated layer fragments with additionally deposited amorphous powders. The fragments could be explained by the sensitivity of the layers against physical treatment (i.e. bending when removing out of the experimental setup) and also could give slightly information about the crystalline character of the layers.

#### Characterization of the deposited layer by profilometry and ellipsometry

To determine the thickness of the SiO<sub>2</sub> layer a trench is etched into the SiO<sub>2</sub> layer. Therefore a photoresist is spun on the layer and photolithographically structured. Afterwards the trench is etched into the SiO<sub>2</sub> layer with a buffered hydrofluoric acid (20 %).

Figure 4 shows the result of a 3D-scan of the trench. The measurement has been carried out with a Tencor P10 Profilometer. The scanned field is 5 mm in depth and 2 mm in width. The resulting thickness of the SiO<sub>2</sub> layer ranges from 350 nm to 700 nm. This results in an average coating rate of 1,6 nm/s.

Additionally the measured values of the 3D-scan are used to calculate the RMS (Root-Mean-Square)-roughness of the surface of the deposited SiO<sub>2</sub>-layer. The RMS-roughness of the SiO<sub>2</sub>-surface is 14,09 nm. This corresponds approximately 2-4 % of the SiO<sub>2</sub>-layer thickness. The

refractive index of  $\text{SiO}_2$  has been determined by ellipsometric measurements with 1,476 showing a good accordance with the literature value of 1,460 for thin films [22].

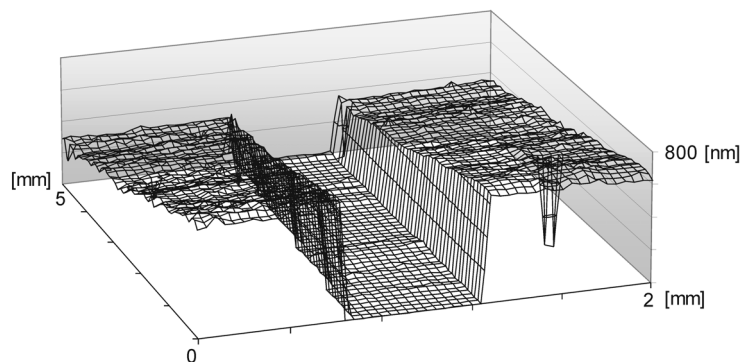


**Figure 4.** 3D-scan of a trench in the  $\text{SiO}_2$  layer recorded with a profilometer.

### Characterization of the deposited layers with IR-spectroscopy

In order to obtain IR transmission spectra of the deposited layers roughly independent from the substrate an attenuated total reflection (ATR) unit shown in figure 5 is applied.



**Figure 5.** Schematic view of an attenuated total reflection (ATR) unit.

To obtain the transmission spectrum the absorption spectra of the bare and coated substrate are measured. Each absorption spectrum of the deposited substrate is divided by the bare one leading to the characteristic spectra shown in figure 6 with the Si-O-Si specific peak at  $1100\text{ cm}^{-1}$ . The spectrum also shows a pressure and buffer gas dependent growth. Apparently the ratio between oxygen and tetraethoxysilane and also the applied buffer gas play a significant role in the deposition mechanisms.

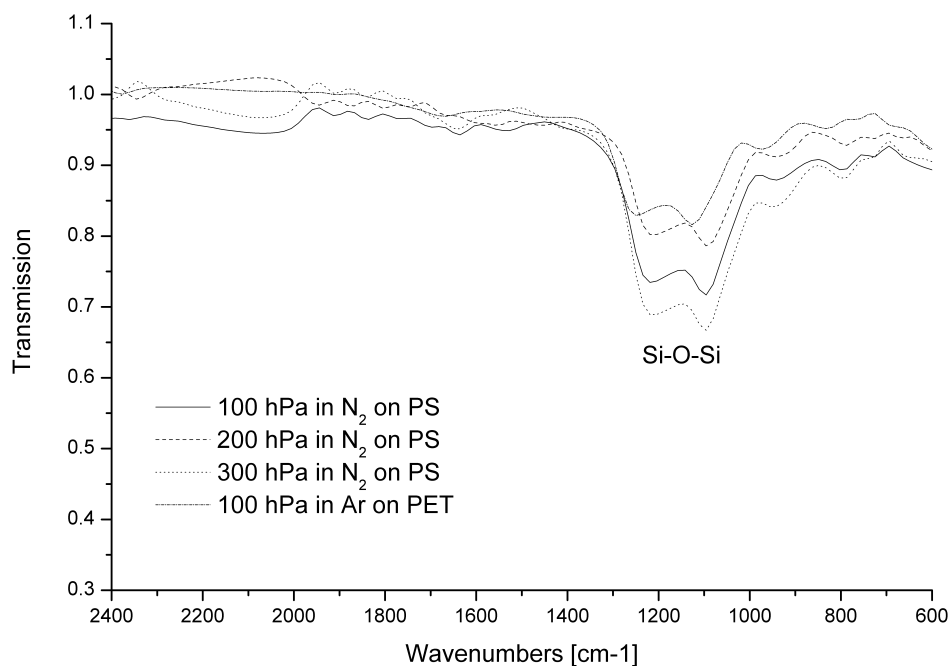


**Figure 6.** Infrared spectroscopy results with an attenuated total reflection (ATR) unit.

## Non-thermal Plasma Characteristics

The universal voltage-current characteristics shown in figure 7 illustrate the pathway of a DC discharge from the dark discharge via the glow discharge to the arc discharge regime. The experimental obtained voltage-current characteristics presented in figure 8 at atmospheric pressure in argon fully obey the different regime dependencies.

The experimental voltage-current characteristic of helium and neon at atmospheric pressure shows similar ignition behaviour. Thus, the MSE generated plasma operates as a glow discharge at atmospheric pressure in all mentioned gases. The transition to the arc discharge regime could be illustrated by the U-I characteristics and the optical emission spectra as well.

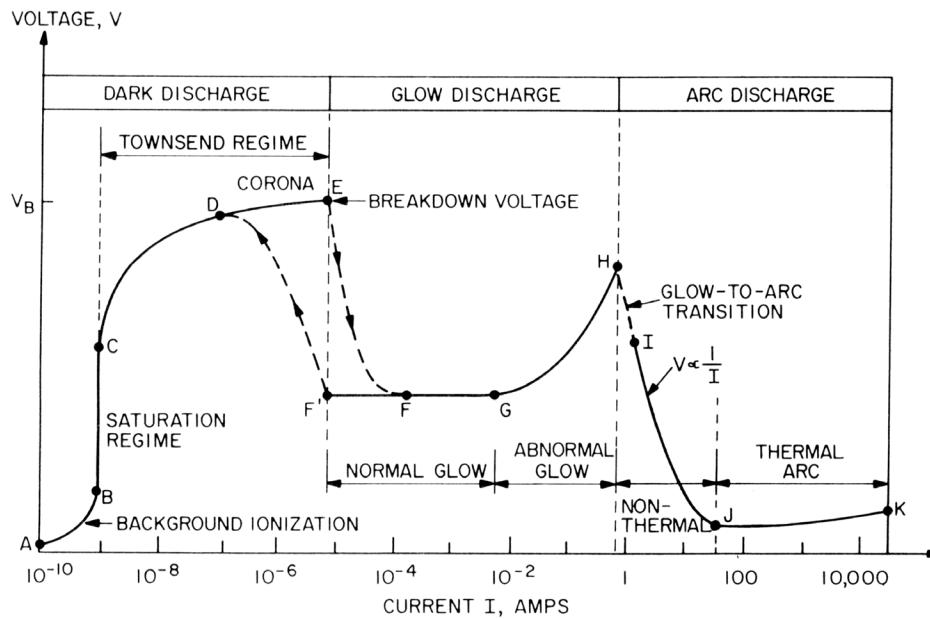
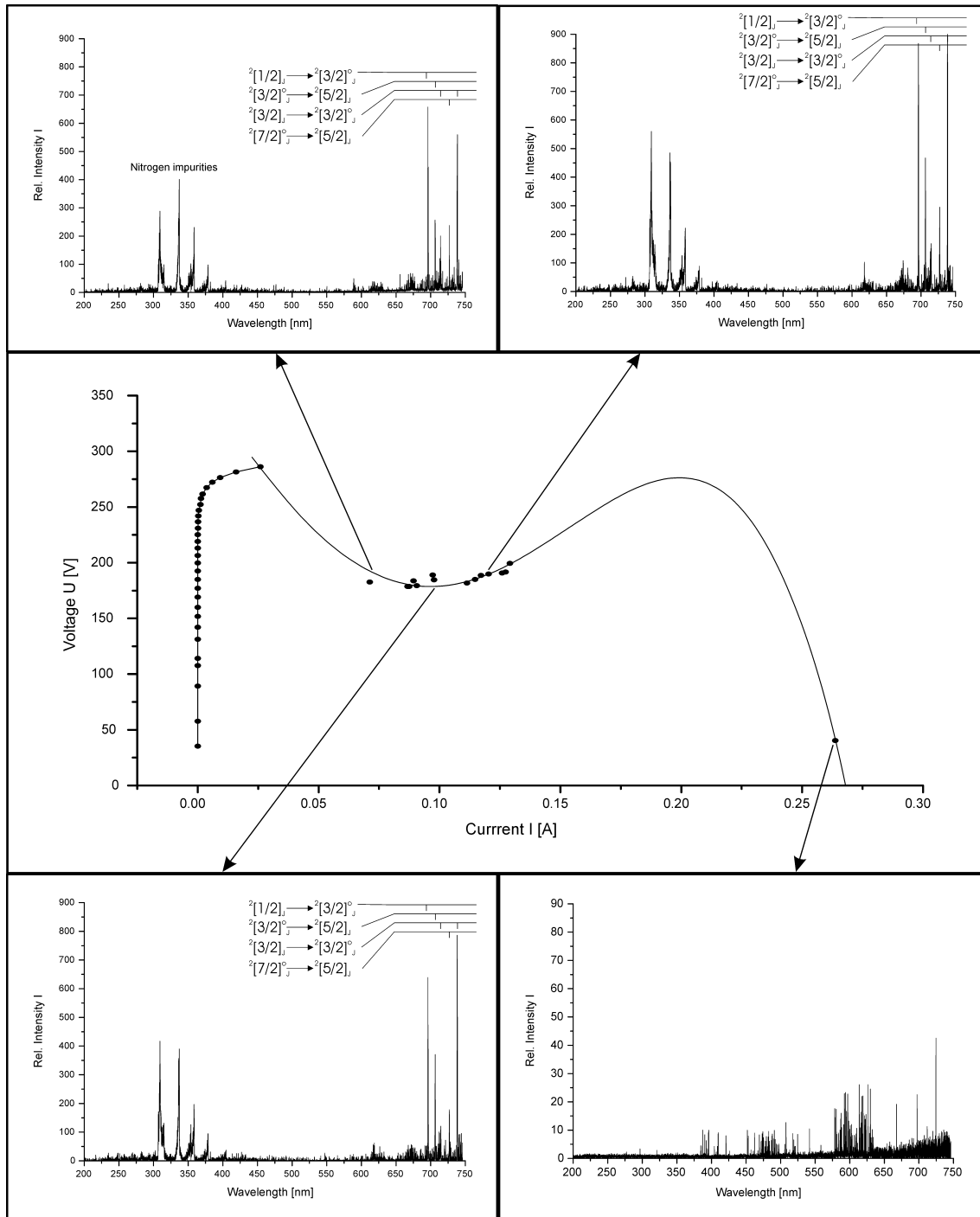


Figure 7. Universal voltage-current characteristics of a DC discharge [23].



**Figure 8.** Experimental U-I characteristics combined with optical emission spectra at 1000 hPa in argon.

## Conclusion

We show the processing of MSE arrays by means of modern micromachining, including high-aspect-ratio lithography and micro electroforming. These high performance MSE arrays are capable to induce plasma at high pressures up to atmospheric pressure. Plasma chemistry for deposition processes with a high application potential can already be induced up to 600 hPa, leading to homogenous SiO<sub>2</sub> layers on PS, PET, silicon and copper, while PP shows too poor adhesion. Thermal damages of the substrates were not observed.

## References

1. F. Massines, A. Rabehi, P. Decomps, R. Ben Gadri, P. Ségur, C. Mayoux, "Experimental and theoretical study of a glow discharge at atmospheric pressure controlled by dielectric barrier", *J. Appl. Phys.*, 83 (1998), 2950-2957
2. F. Massines, P. Ségur, N. Gherardi, C. Khamphan, A. Ricard, "Physics and chemistry in a glow dielectric barrier discharge at atmospheric pressure: diagnostics and modelling" *Surf. Coat. Technol.*, 174-175 (2003), 8-14
3. S. Okazaki, M. Kogoma, M. Uehara, Y. Kimura, "Appearance of stable glow discharge in air, oxygen and nitrogen at atmospheric pressure using a 50 Hz source", *J. Phys. D: Appl. Phys.*, 26 (1993), 889-892
4. T. Yokoyama, M. Kogoma, T. Moriwaki, S. Okazaki, "The mechanism of the stabilisation of glow plasma at atmospheric pressure", *J. Phys. D: Appl. Phys.*, 23 (1990), 1125-1128
5. D. Trunec, A. Brablec, J. Buchte, "Atmospheric pressure glow discharge in neon", *J. Phys. D: Appl. Phys.*, 34 (2001), 1697-1699
6. K. Kelly-Wintenberg, A. Hodge, T. C. Montie, L. Deleanu, D. Shermann, J. Reece Roth, P. Tsai, L. Wadsworth, "Use of a one atmosphere glow discharge plasma to kill a broad spectrum of microorganisms", *J. Vac. Sci. Technol.*, 17 (1999), 1539-1544
7. J. Park, I. Henins, H. W. Hermann, G. S. Selwyn, "Gas breakdown in an atmospheric pressure radio-frequency capacitive plasma source", *J. Appl. Phys.*, 89 (2001), 15-19
8. J. Park, I. Henins, H. W. Hermann, G. S. Selwyn, "Discharge phenomena of an atmospheric pressure radio-frequency capacitive plasma source", *J. Appl. Phys.*, 89 (2001), 20-28
9. R. H. Stark, K. H. Schoenbach, "Direct current high-pressure glow discharge", *J. Appl. Phys.*, 85 (1999), 2075-2080
10. R. H. Stark, K. H. Schoenbach, "Direct current glow discharges in atmospheric air", *Appl. Phys. Lett.*, 74 (1999), 3770-3772
11. C. Penache, A. Bräuning-Demian, L. Spielberger, H. Schmidt-Böcking, "Experimental study of high pressure glow discharges based on MSE arrays", *Proceedings of the Seventh International Symposium on High Pressure Low Temperature Plasma Chemistry (HAKONE VII)*, Greifswald (2000), 501-505
12. J. G. Eden, S.-J. Park, N. P. Ostrom, S. T. McCain, C. J. Wagner, B. A. Vojak, J. Chen, C. Liu, P. von Allmen, F. Zenhausern, D. J. Sadler, C. Jensen, D. L. Wilcox, J. J. Ewing, "Microplasma devices fabricated in silicon, ceramic, and metal/polymer structures: arrays, emitters and photodetectors", *J. Phys. D: Appl. Phys.*, 36 (2003), 2869-2877
13. S.-J. Park, C. J. Wagner, C. M. Herring, J. G. Eden, "Flexible microdischarge arrays: Metal/polymer devices", *Appl. Phys. Lett.*, 77 (2000), 199-201

14. C. Geßner, P. Scheffler, K.-H. Gericke, "Characterisation of a novel micro-structured plasma source via optical emission and laser induced fluorescence spectroscopy", *Proceedings of the Seventh International Symposium on High Pressure Low Temperature Plasma Chemistry (HAKONE VII)*, Greifswald (2000), 112-116
15. H. Schlemm, D. Roth, " Atmospheric pressure plasma processing with microstructure electrodes and microplanar reactors", *Surf. Coat. Technol.*, 142-144 (2001), 272-276
16. K.-H. Gericke, C. Geßner, P. Scheffler, "Micro-structure electrodes as means of creating uniform discharges at atmospheric pressure" *Vacuum*, 65 (2002), 291-297
17. C. Geßner, P. Scheffler, K.-H. Gericke, " Micro-structured electrode arrays - low-temperature discharges at atmospheric pressure", *Proceedings of the International Conference on Phenomena in Ionized Gases (XXV ICPIG)*, Nagoya, 4 (2001), 151-152
18. L. Baars-Hibbe, P. Sichler, C. Schrader, C. Geßner, K.-H. Gericke, S. Büttgenbach, "Micro-structured electrode arrays: atmospheric pressure plasma processes and applications", *Surface and Coatings Technology*, 174-175 (2003), 519-523
19. L. Baars-Hibbe, C. Schrader, P. Sichler, T. Cordes, K.-H. Gericke, S. Büttgenbach, S. Draeger, "Micro-structured electrode arrays : high frequency discharges at atmospheric pressure – Characterization and new applications", *Surface and Coatings Technology*, 174-175 (2003), 519-523
20. J. O'Brien, P.J. Hughes, M. Brunet, B. O'Neill, J. Alderman, B. Lane, A. O'Riordan, C. O'Driscoll, "Advanced photoresist technologies for Microsystems", *Journal of Micromechanics and Microengineering*, 11 (2001), 353-358.
21. H. Lorenz, M. Despont, N. Fahrni, N. LaBianca, P. Renaud and P. Vettiger, "SU-8: a low cost negative resist for MEMS", *Journal of Micromechanics and Microengineering*, 7 (1997), 121-124.
22. Aicha A. R. Elshabini-Riad, Fred D. Barlow III, *Thin Film Technology Handbook*, (New York, NY: McGraw-Hill, 1997), 8-35
23. J. Reece Roth, "Industrial Plasma Engineering", *Institute of Physics*, 1 (1995), 353